Journal of Applied Fluid Mechanics, Vol. 18, No. 1, pp. 60-72, 2025.
Available online at www.jafmonline.net, ISSN 1735-3572, EISSN 1735-3645.
https://doi.org/10.47176/jafm.18.1.2853

Optimal Design and Analysis of the Cooled Turbine Blade in Gas Turbines with CFD

E. Yildiz[1], F. Koca[2†] and I. Can[2]

[1] *Institute Science, Sivas Cumhuriyet University, Sivas, 58100, Turkey*
[2] *Technology Faculty, Sivas Cumhuriyet University, Sivas, 58100, Turkey*

†Corresponding Author Email: ferhatkoca@cumhuriyet.edu.tr

ABSTRACT

In this study, the effects of the structural geometries of the channels used for cooling blades in the heated regions of the gas turbine exposed to high temperature were investigated. It is aimed to cool the gas turbine blade using 10 different types of ribbed channels by simulation method. Roof, inverted roof, slope and wedge ribs with standard and stepped arrangements developed for improving thermal performance in a rectangular cooling duct with a 4:1 ratio aspect were studied. Square type rib, the basic geometry is designed to make thermal comparisons. Details of turbulent flow and numerical calculations were made using of the standard k-ε turbulence model by means of the Computational Fluid Dynamics (CFD) method. The heat transfer in ribbed walls was examined in four different Reynolds numbers, 10000, 20000, 40000 and 80000 according to the channel input cross section. As a result of the calculations, the temperature changes of the turbine blade depending on Re number, the heat transfer improvement occurring in the internal channels inside the blade and the overall thermal performance were compared. The different types of rib evaluated in the study were compared with the standard-square rib; higher Nu number was obtained in stepped-wedge rib, stepped-roof rib, stepped-slope rib and stepped-inverted roof rib, respectively. It has been observed that a stepped-wedge rib can improve overall thermal performance and is promising for internal turbine blade cooling applications. The best operating range of all models was found to be between Re=40000 and Re=80000. The highest PEC results were obtained in the stepped-wedge rib model. This is 3.37% higher than the closest performing stepped-inverted roof rib model with 5.04 at Re=8000.

Article History

Received May 18, 2024
Revised July 8, 2024
Accepted August 3, 2024
Available online November 6, 2024

Keywords:

Gas turbines
Blade cooling
Computational fluid dynamic
Rib
Optimization

1. INTRODUCTION

Energy resources are limited in our world, so it requires efficient use of available resources. The development of gas turbines used in the aviation industry and electric power generation sectors is in the direction of increasing efficiency and power as well as reducing operating and manufacturing costs (Sunden & Xie, 2010). The studies carried out by the manufacturers to meet these targets are generally on combustion technologies, materials and cooling systems. Since most of the engine failures are related to blade failures, cooling of the blades is important for safe operation. As this causes a reduction in the thermal efficiency and power output of the engine, understanding and optimization of the cooling technology for the turbine blade geometry under engine operating conditions is important. As the turbine inlet temperature increases, the temperature to which the blades are exposed also increases and the material, design and coating properties of the blades change due to this thermal increase. As a result of these effects, deformations such as fatigue, corrosion and crack formation occur in the blades, which reduces the overall service life of gas turbines. With the developing gas turbine technology, the operating temperatures of the turbines have also increased and the aerothermal and structural loads to which the parts in the hot parts are exposed have gained great importance in terms of the operating efficiency, operating life and safety of the engine. Increasing the temperature resistance of turbine parts with the material structure is limited both in terms of cost and technology. Therefore, high temperature resistance of turbine blades can only be achieved by improving the cooling systems (Han, 2004; Apostolidis, 2015).

NOMENCLATURE

A	channel inlet area	p	rib pitch
D_h	hydraulic diameter	q	heat flux
f	friction coefficient	Re	Reynolds number
k	conductivity	w	rib height
Nu	Nusselt number	T	temperature
h	penetration depth	u	fluid velocity
ΔP	pressure drop	μ	dynamic viscosity
ρ	fluid density	PEC	Performance Evaluation Criteria

Internal cooling in gas turbines or blade cooling of gas turbines is a topic of great interest to researchers (Lacovides & Launder, 1995; Horlock et al., 2001; Apostolidis, 2015; Bredberg, 2002; Sunden & Xie, 2010; Han, 2013; Nagaiah & Geiger, 2014). In the literature, there are many studies that aim to design better heat transfer structures by using different rib models or arrangements in the duct for the wing (Kim et al., 2009; Chung et al., 2015; Abraham & Vedula, 2016; Singh & Ekkad, 2017; Liu et al., 2021; Zhang et al., 2021).

Abdel-Moneim et al. (2021) experimentally investigated turbulent heat transfer and flow friction characteristics in a horizontal rectangular duct with an aspect ratio of 1:4 with multiple zigzag (V-shaped) ribs arranged at the bottom. They observed that multiple V-shaped ribs increase turbulence and provide a significant increase in heat transfer while increasing flow friction. Alfarawi et al. (2017) conducted experimental investigations at a Reynolds number between 12500 and 86500, aiming to increase heat transfer through a rectangular duct roughened with hybrid ribs. They stated that the increase in heat transfer is critically affected by the flow velocity and turbulence intensity as well as the rib slope/height (p/e) ratio. Du et al. (2020) aimed to improve the thermal performance in a labyrinth duct with different rib shapes. They performed calculations for rectangular, curved and trapezoidal rib models at Reynolds numbers between 10000 and 50000. They performed numerical calculations for rectangular, curved and trapezoidal rib models at Reynolds numbers between 10000 and 50000 using ANSYS. They observed that the curved rib gives high Nusselt number and friction factor. Liu et al. (2018a) applied fractal theory to the design of cut ribs in the internal cooling of a gas turbine blade. They designed a rectangular duct with truncated ribs inserted in the lower wall. They focused on the symmetries of ribbed channels with two-sided truncated ribs, three-sided truncated ribs and five-sided truncated ribs. They compared the thermal performance for all roughened ducts considering both heat transfer and pressure drop. Turbulent flow details were presented by numerical calculations with k-ω SST. From the experimental results, they found that the fractal truncated ribs with smaller length scales have greater heat transfer at low Reynolds numbers. In another study, to improve thermal performance in a rectangular cooling channel with a 4:1 aspect ratio, Liu et al. (2021) focused on perforated 90° ribs. The heat transfer of ribbed walls was investigated experimentally and numerically at Reynolds numbers 40000 and 80000. They observed that compared with normal ribs, the low heat transfer behind the ribs is improved by perforated ribs with low pressure loss. In more recent work, Zheng et al. (2023) attempted to develop a new hierarchical rib arrangement scheme aimed at improving cooling efficiency. Based on the uniform scheme, they applied hierarchical scheme to six representative rib configurations (angled, transversed, M-type, inverted M-type, V-type and inverted V-type ribs) and evaluated for its applicability and generality. They found that the hierarchical scheme for all rib configurations can significantly reduce friction loss as desired, with a reduction of up to 50% for the inverted V-shaped rib in particular. Finally, it is reported that for all ribs evaluated, the hierarchical scheme can improve the overall performance factor by more than 10% and up to 21.15% for the V-shaped rib. Tanda et al. (2023) studied the natural convective heat transfer from a ribbed vertical plate in an experimental setting, varying the size and pitch of the ribs, and considering the effect of the rib cut. These changes were studied in the range of the surface temperature Rayleigh number (Ra) of the base plate from 3.4×10^8 to 4.9×10^8, revealing the main differences. As a result, they obtained the optimum rib segment length for truncated ribs. Jaiswal and Afzal (2023) carried out the design of truncated prismatic ribs in a rectangular duct in a proxy-based optimization framework at a fixed Reynolds number (Re = 42500). For optimization, they determined three design variables, e/D_h, p/e and ep/e, which are rib ratios according to hydraulic diameter, pitch and cutting height. Compared to the reference design, they reported an optimal design with a relative thermal performance improvement of 168.60%. Ris et al. (2024) considered ribbed duct as a model of the cooling system for a gas turbine blade. They numerically analyzed the heat and flow transfer at a variable Reynolds number between 5×10^4 and 2×10^5 and a constant Prandtl number of 0.7. They placed square ribs with a ratio of 10% to the channel height at an angle of 45° to the longitudinal axis of the channel. They compared the numerical data with the experimental results and reported that the numerical method was in good agreement. In this respect, the numerical data were found to be reliable.

Typical ribbed channels and their thermal performances, which have been the subject of research in recent years, are listed in a table in Liu et al. (2021). The basic channel and standard square rib used in the study were designed in accordance with the literature, and the other models were varied in accordance with the basic dimensions. In the studies encountered in the literature, only rib geometric change, only Re number change or only rib cross-sectional change was considered. This study analyses these three variables together and reveals the effects on each other. Thus, it is aimed to extend the literature.

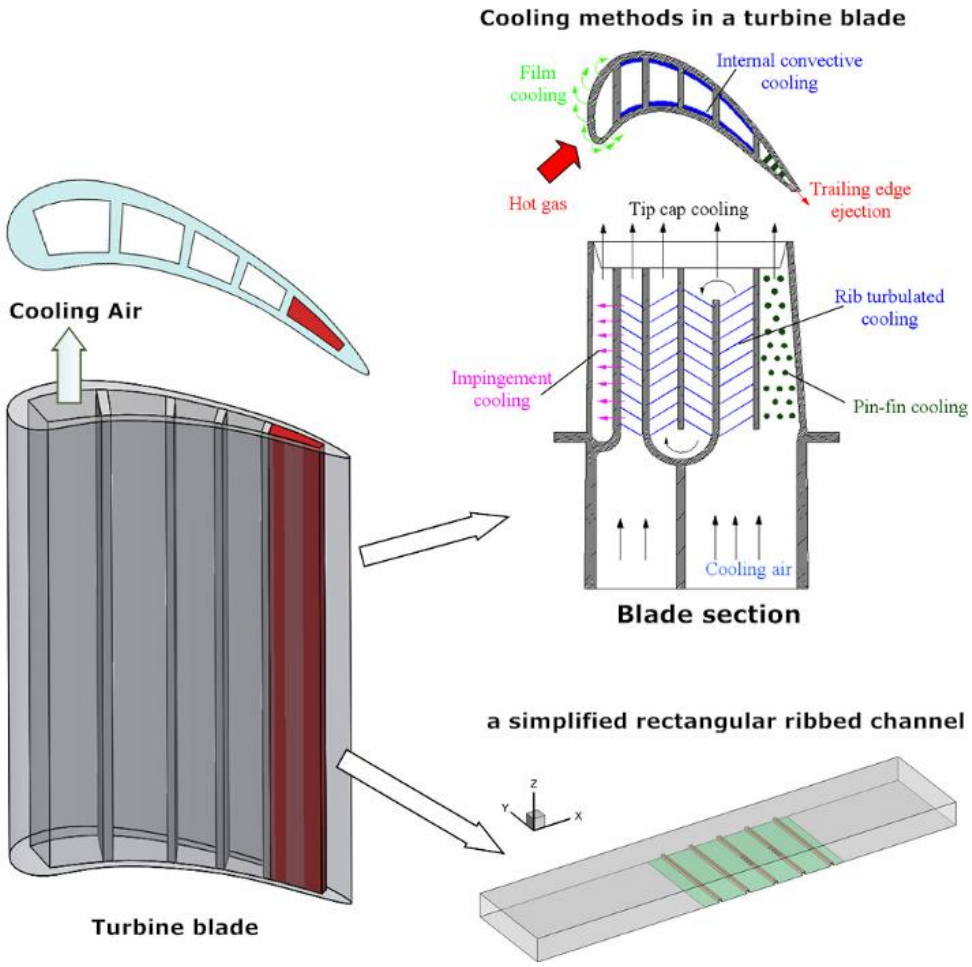

Fig. 1 Ribbed ducts in the internal cooling of a turbine blade (Liu et al., 2021)

In this study, the optimum design and analysis of the cooled turbine blade in gas turbines were carried out using ANSYS-Fluent package program, which is a CFD application. In order to improve efficiency in gas turbines, it is intended to improve heat transfer through the use of ribs in a part of the flow area of the blade. Calculations were performed for different Reynolds numbers of the fluid and different rib geometries. Consequently, the cooling performances of gas turbine blades were investigated by analyzing the heat transfer structures in models with different geometries.

2. MATERIAL AND METHOD

In this study, ribbed channels were used for cooling a turbine blade. The channel and calculation area analyzed for the improvement of heat transfer in the gas turbine blade are shown in detail in Fig. 1. The calculation area is a rectangular cooling channel with an aspect ratio of 4:1 with ribs placed on the lower walls. The length (L), width (W) and height (h) of the calculation area are 1500 mm, 320 mm and 80 mm respectively. The bottom wall of the center part of the channel is the surface where the heat flux is applied and all surfaces except the surface where the heat flux is applied are considered insulating. Fluid velocity and temperature were assumed constant at the channel inlet. The study was carried out between 10000 and 80000 values of Re number calculated according to the channel inlet cross section. The standard k-ε turbulence model was used as the turbulence model and air was used as the fluid. The inlet temperature of the air into the system was assumed to be 300 K, incompressible, fully developed, dry and constant thermo-physical properties. In addition, zero pressure was considered at the outlet section.

In the study, five different rib structures named as square, roof, inverted roof, slope and wedge were used for two different arrangements, standard and stepped. The first arrangement was specified as a continuous piece and was referred to as a standard rib. The length, width and height of the ribs are 320 mm, 10 mm and 10 mm respectively. The distance between the ribs (equal distance of each rib to each other) is 100 mm. The second arrangement was defined as a truncated piece and was called a stepped rib. The difference from the standard rib is that the rib is cut by 25% of its total length. The first rib is in the center of the channel and is 240 mm long. The second rib is in the form of 2 pieces and the gap distance between them is 80 mm. The width and height of the ribs are 10x10 mm, respectively, as in the standard model and five different rib geometries were designed according to both arrangements. In order to compare the numerically calculated results with the model designed by Liu et al. (2018b), the first rib geometry was designed as square. Also the square rib has a width and height of 10x10 mm.

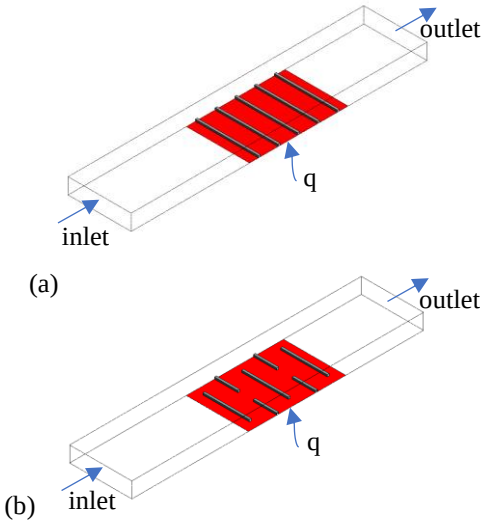

Fig. 2 Rib arrangement methods a) standard b) stepped

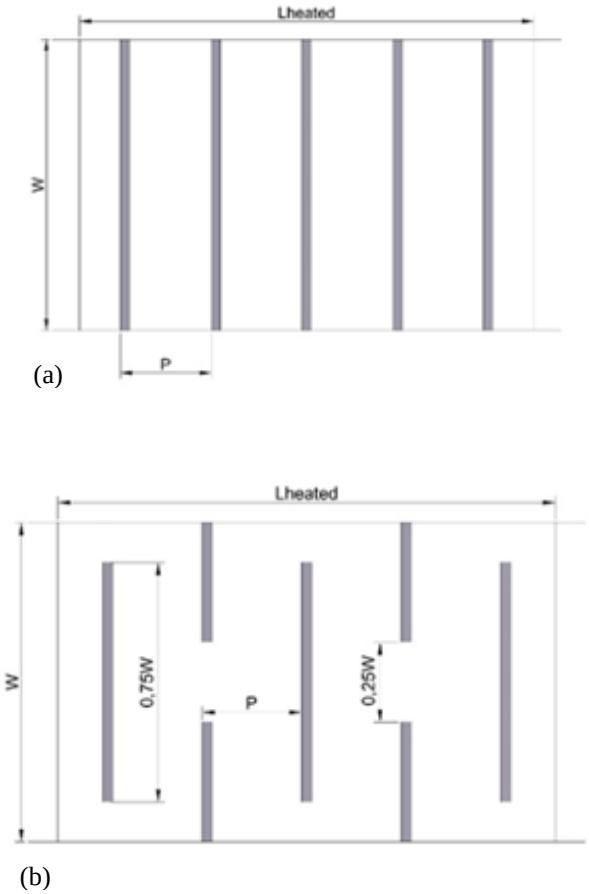

Fig. 3 Dimensions of arrangement methods a) standard b) stepped

Figure 2 shows the different rib arrangements used in the study and Fig. 3 shows the dimensions of these arrangements.

In order to better understand the designs, the dimensions for each model are given in Table 1.

Table 1 Geometrical dimensions of the models

Symbols	*W*	*L*	$L_{heatedsurface}$	D_h	*e*	*P*
Values (mm)	320	1500	500	128	10	100

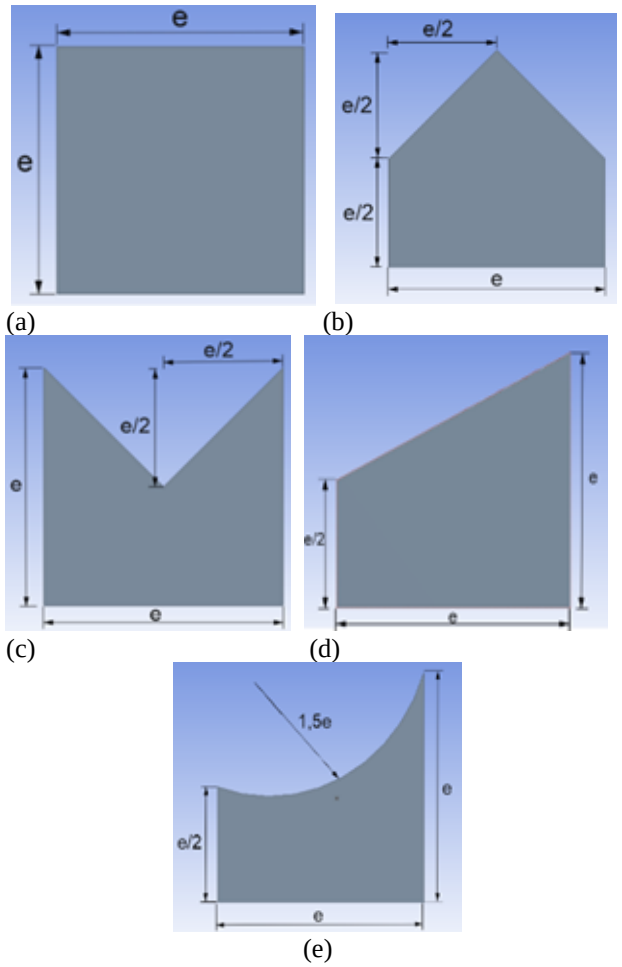

Fig. 4 Structures and dimensions of used rib models (a) square (b) roof (c) inverted roof (d) slope (e) wedge

When all models were designed with both arrangements (standard and stepped), a total of 10 different designs were obtained. All models used in the study are shown in detail in Fig. 4.

The basic geometry used in the study is based on Liu et al. (2018b). The rectangular duct with 4:1 inlet cross-section consists of 3 parts as inlet, test area and outlet as shown in Figure 2. The duct wall surfaces outside the inlet and outlet sections were assumed to be adiabatic, while a constant surface heat flux of 1000 W/m^2 was applied to the lower surface of the test area where the ribs were located.

The geometrical structure and boundaries from the referenced paper (Liu et al., 2018b) were used to validate the numerical study. Since the calculation results are different with various turbulence models, a suitable model should be selected for CFD simulation of turbulent flow

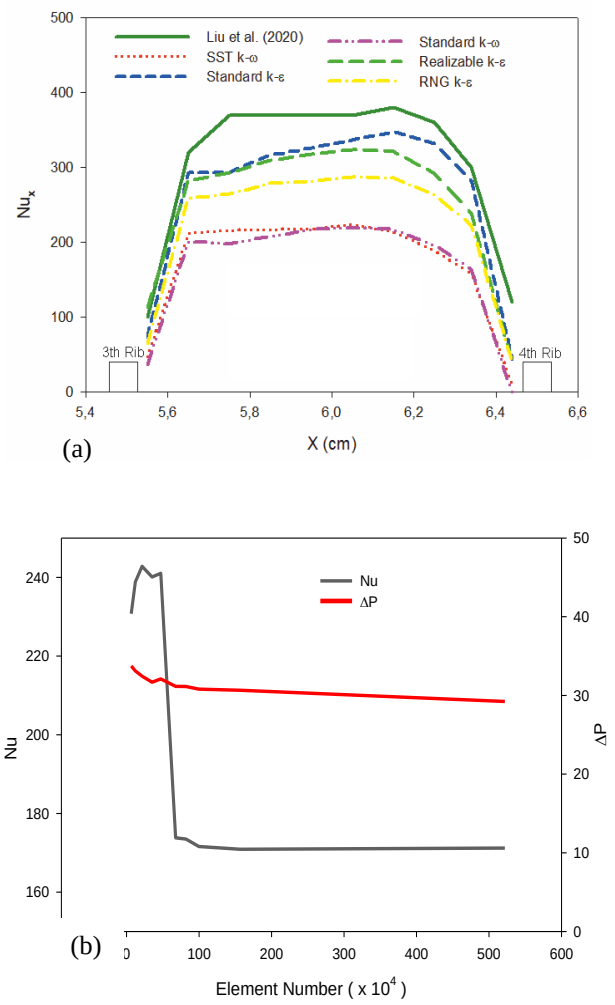

Fig. 5 a) Nu_x-x plot of the ribbed channel model of Li et al. (2020) and different types of turbulence model analyses of the studied ribbed channel b) mesh independence

and heat transfer. In order to obtain the most appropriate turbulence model for the study, five different turbulence models, namely standard k-ε, realizable k-ε, RNG k-ε, standard k-ω and SST k-ω models, were tested and compared for the distribution of the local Nusselt number (Nu_x) of the presented ribbed channel along the flow direction between the 3rd and 4th row ribs at Reynolds number 80000. Figure 5 shows the Nu_x-x plot of the ribbed channel model of Li et al. (2020) and the newly created ribbed channel model. The Nusselt number results calculated with the standard k-ε model give the closest results compared to other turbulence model values. In addition, it is seen in Fig. 5b that the change in Nu number is minimal for $85x10^4$ element number and above. Considering this situation, the analysis was performed with $100x10^4$ mesh element number.

Figure 6 shows the appearance of the mesh structure used. A triangular mesh structure was used throughout the channel and 5-layer inflation was formed on the ribs, which are the solid-fluid region where thermal interaction occurs.

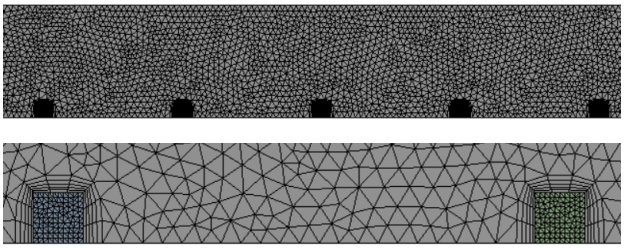

Fig. 6 View of the mesh grid

The basic equations used in this study are the conservation equations for cartesian coordinates and the data equations. Conservation equations are given in Equations 1-5.

Continuity equation:

$$\frac{\partial u}{\partial x}+\frac{\partial v}{\partial y}+\frac{\partial w}{\partial z}=0 \tag{1}$$

Momentum equation in the X direction:

$$\rho\left(u\frac{\partial u}{\partial x}+v\frac{\partial u}{\partial y}+w\frac{\partial u}{\partial z}\right)=-\frac{\partial P}{\partial x}+\mu\left(\frac{\partial^2 u}{\partial x^2}+\frac{\partial^2 u}{\partial y^2}+\frac{\partial^2 u}{\partial z^2}\right) \tag{2}$$

Momentum equation in the Y direction:

$$\rho\left(u\frac{\partial v}{\partial x}+v\frac{\partial v}{\partial y}+w\frac{\partial v}{\partial z}\right)=-\frac{\partial P}{\partial y}+\mu\left(\frac{\partial^2 v}{\partial x^2}+\frac{\partial^2 v}{\partial y^2}+\frac{\partial^2 v}{\partial z^2}\right) \tag{3}$$

Momentum equation in the Z direction:

$$\rho\left(u\frac{\partial w}{\partial x}+v\frac{\partial w}{\partial y}+w\frac{\partial w}{\partial z}\right)=-\frac{\partial P}{\partial z}+\mu\left(\frac{\partial^2 w}{\partial x^2}+\frac{\partial^2 w}{\partial y^2}+\frac{\partial^2 w}{\partial z^2}\right) \tag{4}$$

Energy equation:

$$\left(u\frac{\partial T}{\partial x}+v\frac{\partial T}{\partial y}+w\frac{\partial T}{\partial z}\right)=\alpha\left(\frac{\partial^2 T}{\partial x^2}+\frac{\partial^2 T}{\partial y^2}+\frac{\partial^2 T}{\partial z^2}\right)+\mu\phi \tag{5}$$

Here ρ, μ, α, P and T represent fluid density, viscosity, heat diffusion coefficient, pressure and temperature, respectively.

Dimensionless numbers and related equations are given in Equations 6-11.

$$\mathrm{Re}=\frac{\rho u D_h}{\mu} \tag{6}$$

$$D_h=\frac{4A}{C} \tag{7}$$

$$f=\frac{\Delta P D_h}{2\rho u^2 L} \tag{8}$$

$$Nu=\frac{hD_h}{k} \tag{9}$$

$$h=\frac{q_x}{T_w-T_f} \tag{10}$$

$$PEC=\frac{Nu_{ribbed}/Nu_0}{\left(f_{ribbed}/f_0\right)^{1/3}} \tag{11}$$

Here Re, u, D_h, A, C, L, q_x, T_w, T_f represent Reynolds number, fluid velocity at channel inlet, hydraulic diameter, channel inlet area, channel inlet perimeter, channel length, heat flux, wall temperature, fluid bulk temperature respectively. Also, for the calculation of the PEC number, the ratio of the average values in the new model ribbed structure and the flat channel without ribs was used.

3. RESULTS AND DISCUSSION

The study was carried out for 10000, 20000, 40000 and 80000 values of Re and the pressure contours, turbulence kinetic energy (TKE) contours, velocity vectors, Nu-Re plot, ΔP-Re plot, f-Re plot, TKE-Re plot and PEC-Re plot obtained as a result of the calculations are presented.

The pressure, TKE and velocity contours at lowest Re=10000 are given in Fig. 7a, Fig. 8a and Fig. 9a and at highest Re=80000 are given in Fig. 7b, Fig. 8b and Fig. 9b respectively to illustrate the main differences for the models. In all models, images are given for the plane created in the middle of the channel. In the pressure contours image, the difference in arrangement is clearly demonstrated. High pressure occurred in the upstream regions of the rib and low pressure occurred in the downstream regions. Different rib geometries caused differences in the output data as well as in the TKE and velocity visualizations. For the same Re number, the same legend values are used for a better understanding of the colors. It is clearly seen in the pressure contours that the lowest pressure occurs in wedge and slope models. In turbulence distributions, especially the upper regions of the rib geometries disrupt the flow structure. This situation covers a larger area in staggered models. The velocity contours also support this, creating flow vortices between the ribs, thus contributing to heat transfer through the ribs.

Figure 10 contains the temperature contours for all models for the highest Re number. Rib variation generates different thermal fluctuations. Differences are demonstrated for 300 to 310 K fixed legend scale of the temperature. The difference of temperature fluctuation and heat in the staggered wedge rib model is clearly observed.

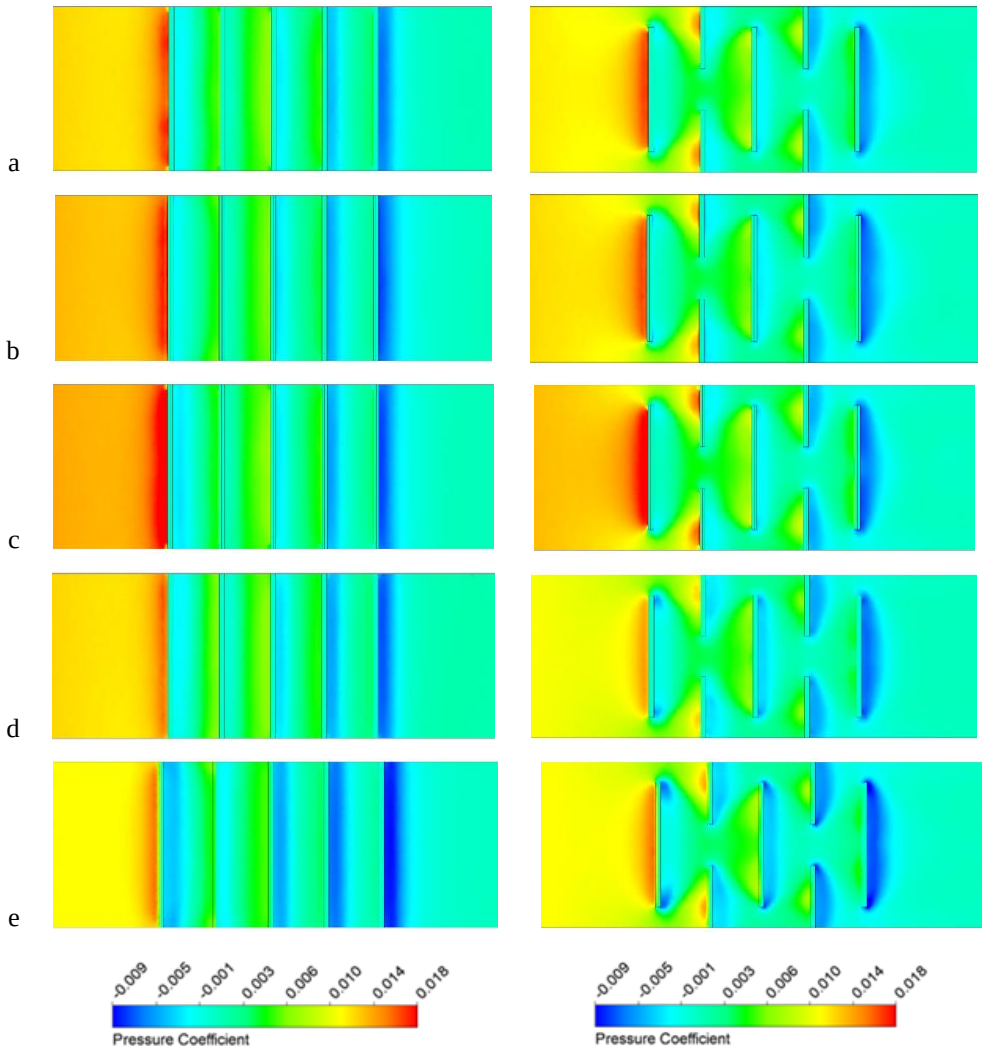

Fig. 7a Pressure contour view of (a) square, (b) roof, (c) inverted roof, (d) slope, (e) wedge structures for standard and stepped rib arrangements at Re=10000

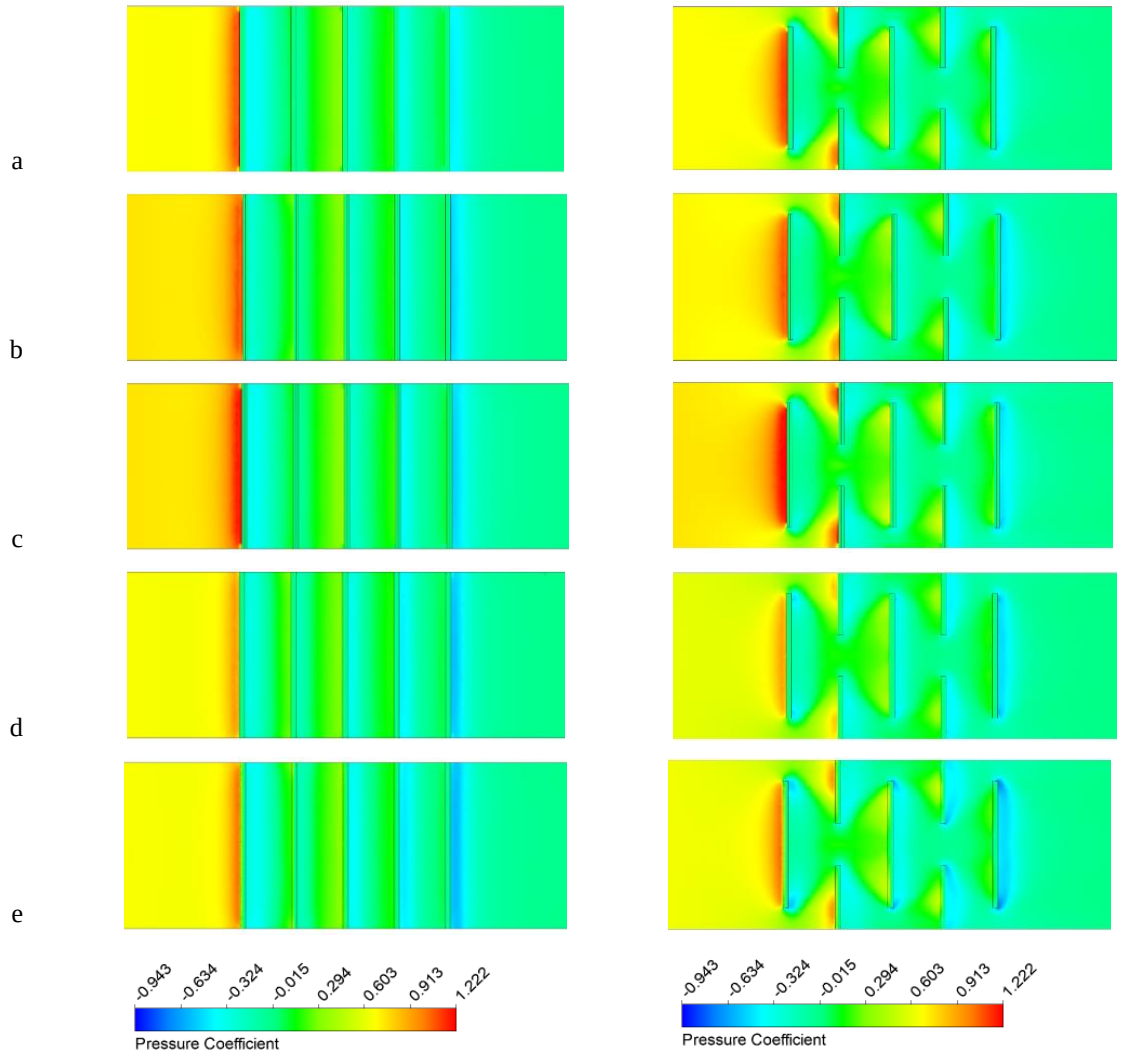

Fig. 7b Pressure contour view of (a) square, (b) roof, (c) inverted roof, (d) slope, (e) wedge structures for standard and stepped rib arrangements at Re=80000

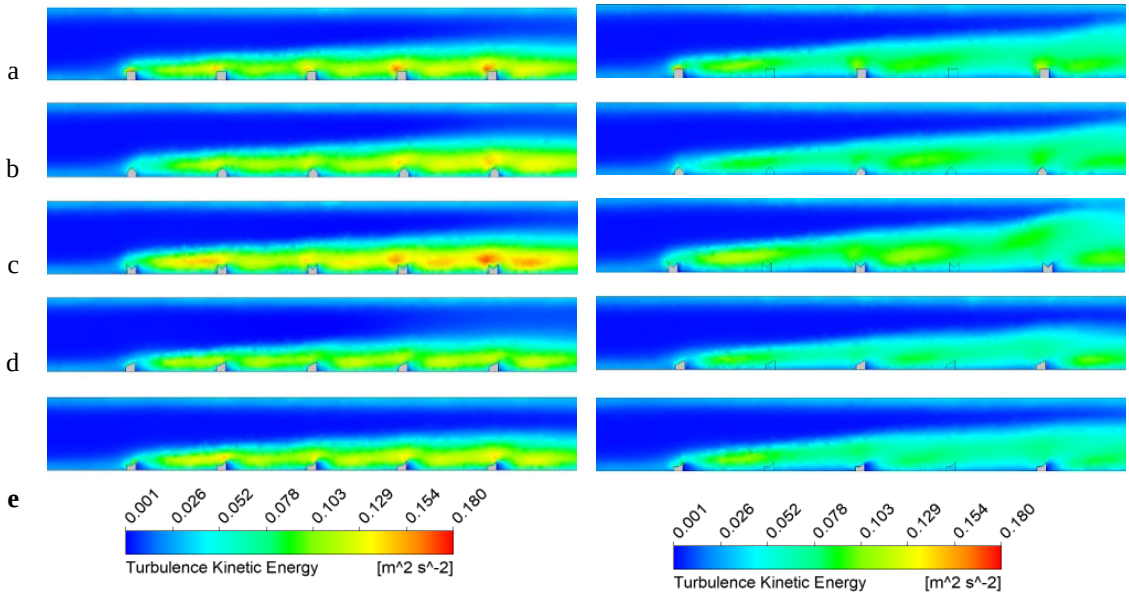

Fig. 8a TKE contours of (a) square, (b) roof, (c) inverted roof, (d) slope, (e) wedge structures for standard and stepped rib arrangements at Re=10000

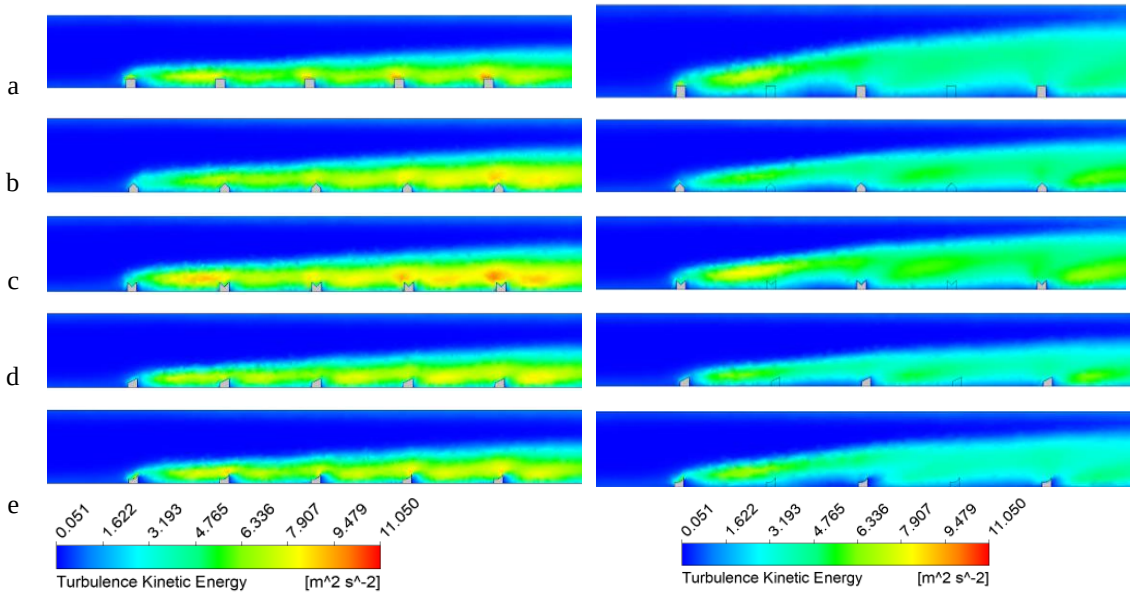

Fig. 8b TKE contours of (a) square, (b) roof, (c) inverted roof, (d) slope, (e) wedge structures for standard and stepped rib arrangements at Re=80000

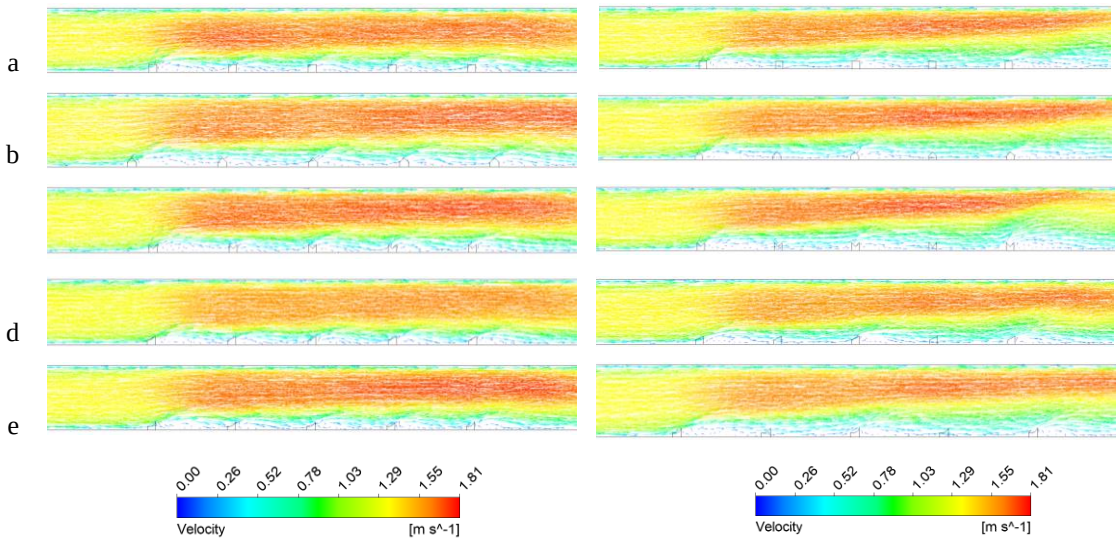

Fig. 9a Velocity vectors for (a) square, (b) roof, (c) inverted roof, (d) slope, (e) wedge structures for standard and staggered rib arrangements at Re=10000

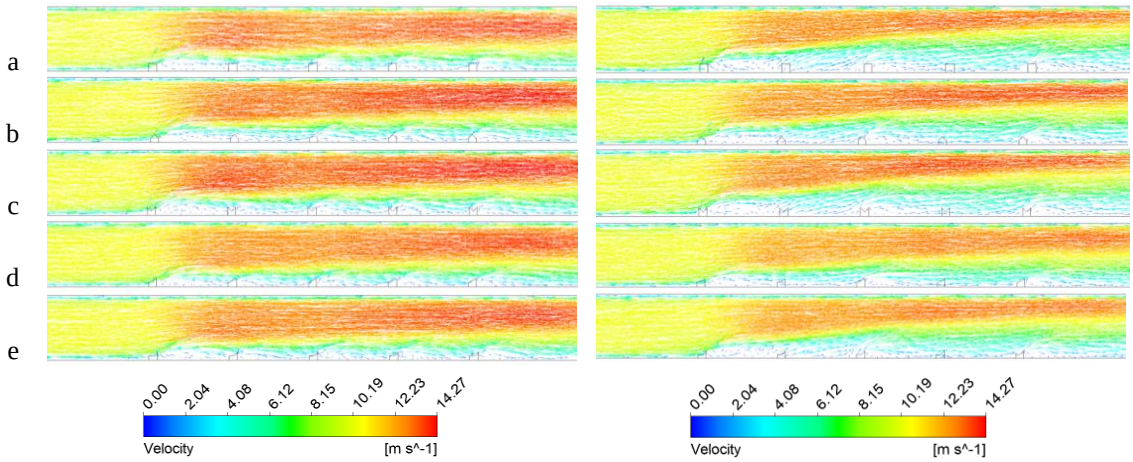

Fig. 9b Velocity vectors for (a) square, (b) roof, (c) inverted roof, (d) slope, (e) wedge structures for standard and staggered rib arrangements at Re=80000

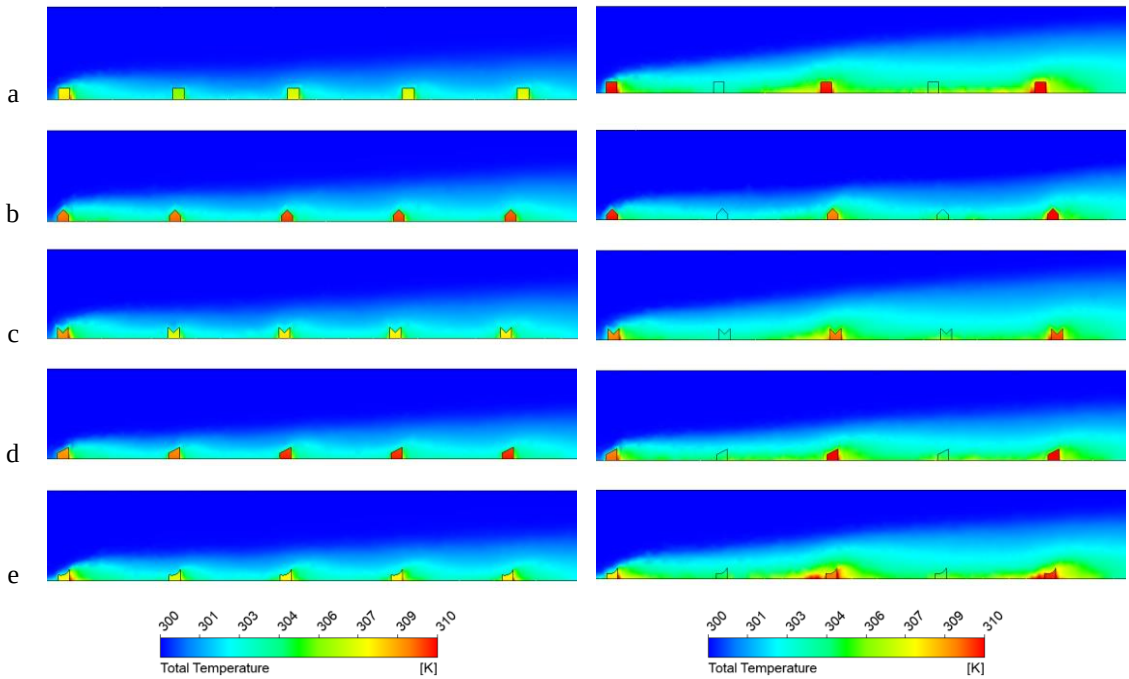

Fig. 10 Temperature contours of (a) square, (b) roof, (c) inverted roof, (d) slope, (e) wedge structures for standard and staggered rib arrangements at Re=80000

The effect of all models on heat transfer at Re values of 10000, 20000, 40000 and 80000 was analyzed by using the data obtained from the calculations. This situation was analyzed with the Nu number, which is considered as one of the most important dimensionless numbers frequently used in heat transfer problems. Figure 11 (a) shows the Re-Nu graph for 10 different types of ribs. Nu number is the ratio of convective heat transfer to conductive heat transfer at the boundary of a fluid as calculated Equation 9. A large Nu number indicates that convectional heat transfer is effective, so it is possible to improve convectional heat transfer by increasing the Nu number. In Figure 11, it is observed that the Nu number increases in each model with the increase in Re number. The effect of this situation on heat transfer is considered to be positive. The Nu values obtained in the square type standard rib model were compared with the other rib models studied. When all the models were compared, the Nu numbers of the stepped rib models were found to be higher and the Nu numbers of the standard type ribs were found to be lower. Since the Nu number is larger in the other models compared to the square rib, it can be said that heat transfer is improved in all models. At Re=40000 and Re=80000, 45.5% and 48.09% higher Nu numbers were obtained in stepped-wedge rib compared to standard-square rib, respectively. The best cooling performances can be achieved by using stepped-wedge, stepped-roof and stepped-slope ribs respectively. If only the standard arrangement is considered, it can be said that the best heat transfer is provided by the use of standard-wedge, standard-roof and standard-slope respectively. In this case, wedge type, roof type and slope type ribs provide better heat transfer than other models. In addition, the difference between the Nu values obtained in the standard-square rib structure and the Nu numbers in the stepped-wedge rib structure clearly revealed that the stepped-wedge rib structure is geometrically more effective.

Figure 11 (b) shows the variation of pressure loss (ΔP) in the system according to Re number for 10 different models. The difference between the inlet and outlet values of the air, which is the working fluid, is considered as pressure loss. It is stated by many researchers in the literature that the increase in ΔP is undesirable. Since the ΔP in the system may require additional pumping power, it can be said to be a factor that reduces efficiency. When all models are analyzed, less ΔP occurs in wedge type and slope type ribs compared to roof type, inverted roof type and square type ribs. The models with less ΔP compared to standard-square type and stepped-square type ribs are stepped-slope rib, stepped-wedge rib, standard-wedge rib and standard-slope rib structures, respectively. At Re= 80000, the ΔP of stepped-wedge rib and stepped-slope rib was 6.30% and 10.22% lower than the standard-square rib, respectively.

The friction factors (f) defined by Equation 8 were compared to evaluate the flow resistance properties of 10 different rib models at different Re numbers. Figure 11 (c) shows the variation graph of the friction factor of different types of rib models with respect to Re number. With the increase in Re number, the f values of all models increase. As the Re number increases, a higher flow resistance occurs. When all models are compared with the standard-square type rib model, it is seen that the lowest coefficient of friction is observed in the standard-inverted roof type rib. The lowest friction coefficient is observed for standard-wedge rib, standard-roof rib, standard-slope rib and stepped-inverted roof rib models respectively. When the f values of the standard-

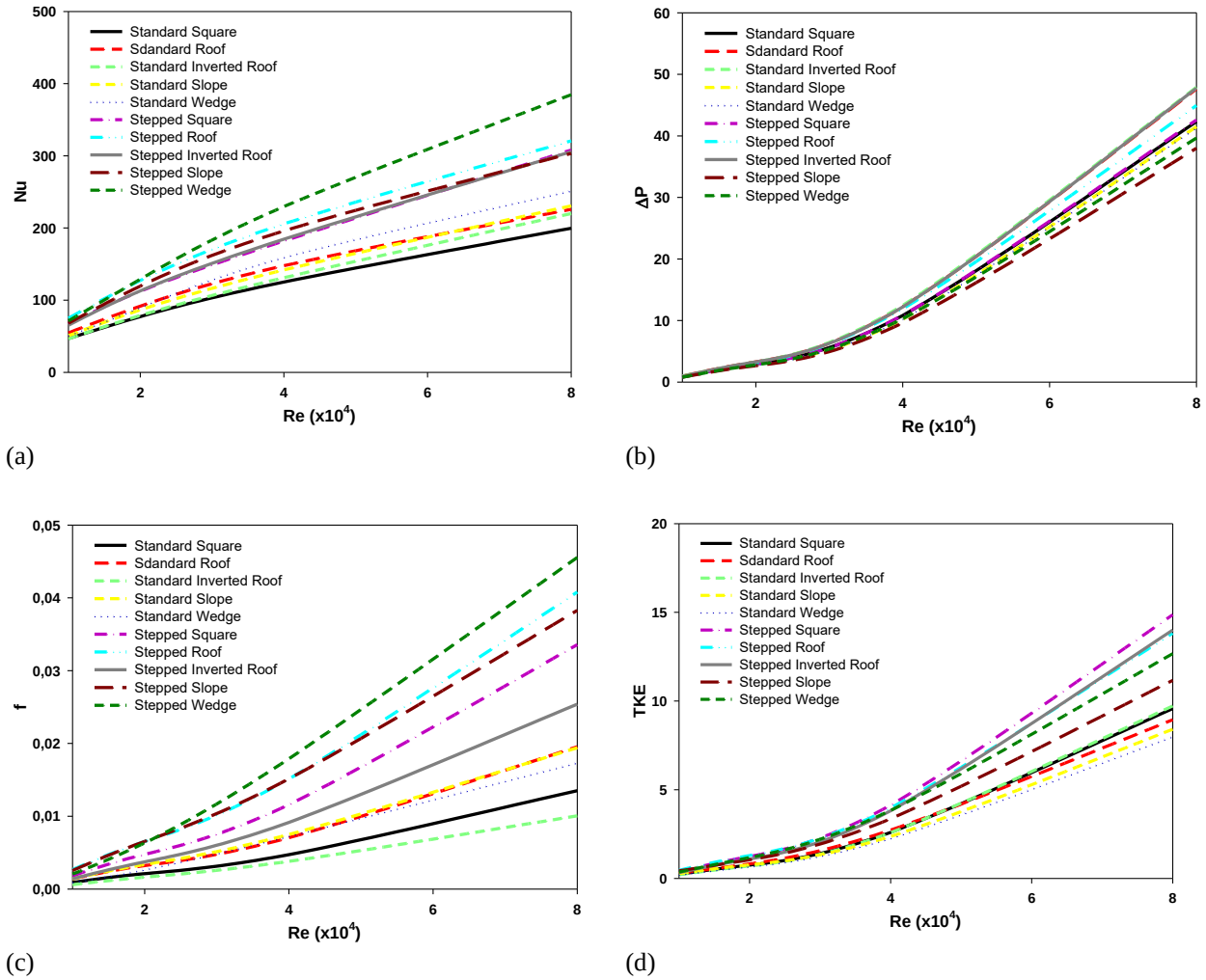

Fig. 11 Variation plot of (a) Nusselt number, (b) Pressure drop (ΔP), (c) friction factor (d) TKE of different rib models according to Reynolds number

inverted roof rib model are examined, it is found that there is 24.21% less friction than the standard-square rib model at Re=40000 and 34.42% less friction than the standard-square rib model at Re=80000. The highest friction coefficient occurs in the stepped-wedge rib model at Re=40000-80000 values. At Re=40000, stepped-slope rib and stepped-roof rib have approximate values. At Re=80000, higher friction occurs in stepped-roof rib than stepped-slope rib. For all Re numbers, the standard-slope rib and the standard-roof rib have approximate values. At Re=10000, Re=20000, Re=40000 values, standard-wedge rib, standard-slope rib and standard-roof rib give approximate values, while at Re=80000 value, 10,64% lower friction values were obtained compared to standard-slope rib and 11,36% lower friction values were obtained compared to standard-roof rib.

Figure 11 (d) shows the variation graph of TKE values according to Re number. In fluid dynamics, TKE is the average kinetic energy per unit mass associated with eddies in turbulent flow. TKE is directly related to the transport of momentum, heat and moisture across the boundary layer. The lowest TKE values are observed in standard-wedge rib, standard-slope rib and standard-roof rib models, respectively. Standard-square rib and standard-inverted roof rib have almost the same values. The highest TKE values are found in stepped-square rib, stepped-inverted roof rib, stepped-roof rib, stepped-wedge rib and stepped-slope rib models, respectively. Stepped-roof rib and stepped-inverted roof rib have 3.80% and 7.67% lower TKE values than stepped-square rib at Re=40000, respectively. At Re= 80000, 6.99% and 5.78% lower TKE values were observed, respectively.

Figure 12 shows the variation graph of PEC number according to Re number. PEC is used to measure thermal performance. It is given in Equation 10 depending on the Nu number and the friction coefficient. The PEC is used to measure how effectively the heat transfer is enhanced in the face of hydrodynamic forces. Therefore, using the PEC number to explain the efficiency of a cooling/heating surface is important. Increased PECs achieved by the application indicate increased heat transfer. In addition, a PEC values greater than 1 is an indication that the heat transfer capacity is higher than the increasing pressure loss (Koca & Güder, 2022, Koca, 2022). Re=40000-80000 is the most effective working range, as can easily be seen from the

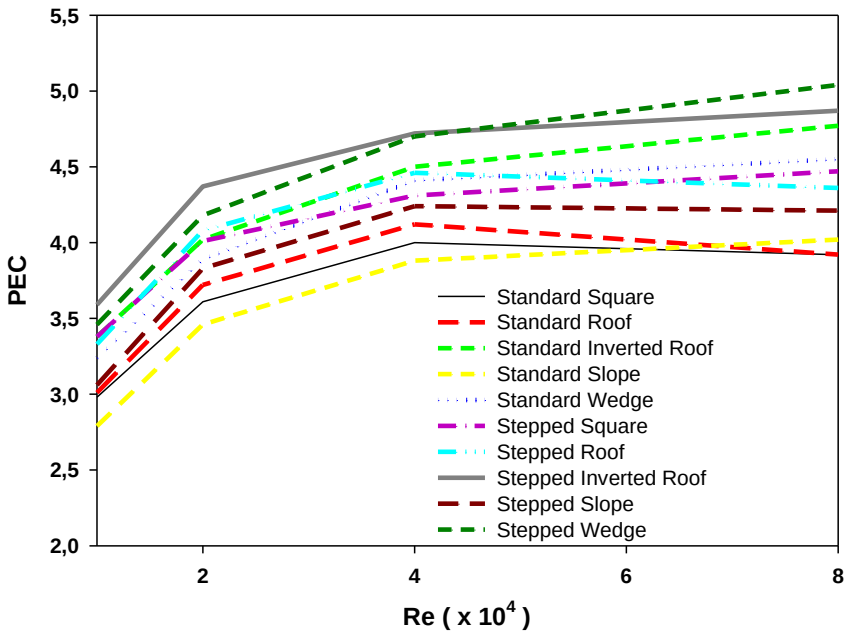

Fig. 12 Variation plot of PEC-Reynolds number for different rib models.

graph. Larger PEC values were obtained at these points compared to other Re numbers. The highest PEC values were measured with stepped-wedge rib, stepped-inverted roof rib, standard-inverted roof rib, standard-wedge rib models, respectively. At Re=40000 and Re=80000, the PEC values of the stepped-slope rib model was greater than the PEC values of the standard-square rib, standard-roof rib and standard-slope rib models. It is also found that at Re=10000 and Re=20000, the stepped-inverted roof rib provides 3.62% and 4.34% higher thermal performance than the stepped-wedge rib, respectively, while at Re=40000, it provides approximately thermal performance. At Re=80000, the stepped-wedge rib provided 3.37% higher thermal performance than the stepped-inverted roof rib. At Re=10000, Re=20000 and Re=40000, the standard-slope rib provided 6.37%, 4.15% and 3% lower PEC numbers than the standard-square rib, respectively. Finally, at Re=80000, standard-roof rib and standard-square rib resulted in 2.48% lower PEC number than standard-slope rib.

4. CONCLUSION

In this study, ribs with different geometries are investigated to improve the thermal performances in a rectangular cooling channel with an aspect ratio of 4:1. It has designed 10 different types of ribbed channels including standard-roof rib, stepped-roof rib, standard-inverted roof rib, stepped-inverted roof rib, standard-slope rib, stepped-slope rib, standard-wedge rib, stepped-wedge rib and standard-square rib, stepped-square rib for comparison. In order to obtain the turbulent flow details, numerical analyses were performed with the standard k-ε turbulence model at Re numbers of 10000, 20000, 40000 and 80000. As a result of the analyses, the comparison parameters are Nu, ΔP, f, PEC values; pressure contours, TKE contours and velocity vectors. In general, the following results were obtained:

- Comparing the standard-square rib with other models, the highest Nu number was provided by stepped-wedge, stepped-roof, stepped-slope and stepped-inverted roof ribs respectively. Rib geometries with standard arrangements have a lower Nu number compared to stepped ribs.

- In terms of pressure drop, stepped-square rib and standard-square rib show almost the same performance compared to others. Compared to these, the models with the best performance are stepped-slope rib, stepped-wedge rib, standard-slope rib and standard-wedge rib, respectively.

- In the comparison of f values, it was found that there was 24.21% less friction for the standard-inverted roof rib model than the standard-square rib model at Re=40000 and 34.42% lower than the standard-square rib model at Re=80000. The highest friction coefficient occurs in the stepped-wedge rib model at Re=40000-80000 values.

- PEC (Performance Evaluation Criterion) values, which are the most significant indicator of the model effectiveness, were computed and it was found that the best operating range of all the models was between Re=40000 to Re=80000. The PEC number of the stepped-wedge rib model at Re=80000 is 3.37% higher than the stepped-inverted roof rib model.

- When all the models are analyzed, it can be said that the models designed with stepped arrangement improve the heat transfer more than the rib models with standard arrangement. It has been observed that the stepped-wedge rib can improve the overall thermal performance and provide more uniform heat transfer areas, promising for applications in the internal cooling of turbine blades. This is due to the variability of the rib

surfaces where the solid-fluid interaction takes place and the rib arrangement changes the contact surface areas and also creates fluid turbulence between the ribs.

- As a result, out of 40 different analyses at 4 determined Re numbers for 5 different models with 2 arrangements, it was found that the heat transfer of the stepped-wedge rib model was most effective in the Re=40000-80000 range and concluded that its use in this range is feasible in comparison to the other models.

ACKNOWLEDGEMENTS

This study was accepted as a master's thesis by Sivas Cumhuriyet University Institute of Science and Technology.

CONFLICT OF INTEREST

The authors declare no conflict of interest.

AUTHORS CONTRIBUTION

Esra Yıldız: Master's Research, Methodology, Validation, Formal Analysis, Investigation, Resources, Writing of the Original Draft; **Ferhat Koca**: Supervising, Methodology, Validation, Formal Analysis, Investigation, Resources, Writing of the Final Manuscript, Review and Editing, Visualization, Text and Figure Formatting; **İbrahim Can**: Supervising, Review and Editing.

REFERENCES

Abdel-Moneim, S. A., Atwan, E.F, & El-Shamy, A.R. (2021, Oct.30th- Nov.1st) Heat Transfer and Flow Friction in a Rectangular Duct with Repeated Multiple v-ribs Mounted on the Bottom Wall, 12th International Mechanical Power Engineering Conference (IMPEC12), pp. 11–25, Mansoura, Egypt. https://feng.stafpu.bu.edu.eg/Mechanical%20Engineering/682/publications/Sayed%20Ahmed%20Abdel-Moneim_V%20Ribs.pdf

Abraham, S., & Vedula, R. P. (2016). Heat transfer and pressure drop measurements in a square cross-section converging channel with V and W rib turbulators. *Experimental Thermal and Fluid Science*, *70*(1), 208–219. https://doi.org/10.1016/j.expthermflusci.2015.09.003

Alfarawi, S., Abdel-Moneim, S. A., & Bodalal, A. (2017). Experimental investigations of heat transfer enhancement from rectangular duct roughened by hybrid ribs. *International Journal of Thermal Sciences*, *118*(August), 123–138. https://doi.org/10.1016/j.ijthermalsci.2017.04.017

Apostolidis, A. (2015). *Turbine cooling and heat transfer modelling for gas turbine performance simulation*. [Ph.D. thesis, Cranfield University School of Engineering] Cranfield, UK. http://dspace.lib.cranfield.ac.uk/handle/1826/9234

Bredberg, J. (2002). *Turbulence modelling for internal cooling of gas turbine blades. department of thermo and fluid dynamics.* [Ph.D. thesis, Chalmers University of Technology] Sweden. https://api.semanticscholar.org/CorpusID:119064306

Chung, H., Park, J. S., Park, S., Choi, S. M., Rhee, D., & Cho, H. H. (2015). Augmented heat transfer with intersecting rib in rectangular channels having different aspect ratios. *International Journal of Heat and Mass Transfer*, *88*(September), 357–367. https://doi.org/10.1016/j.ijheatmasstransfer.2015.04.033

Du, W., Luo, L., Wang, S., Liu, J., & Sunden, B. A. (2020). Enhanced heat transfer in a labyrinth channels with ribs of different shape. *International Journal of Numerical Methods for Heat & Fluid Flow*, *30*(2), 724-741. https://doi.org/10.1108/HFF-05-2019-0393

Han, J. C. (2004). Recent studies in turbine blade cooling. *International Journal of Rotating Machinery*, *10*(6), 443–457. https://doi.org/10.1155/S1023621X04000442

Han, J. C. (2013). Heat transfer augmentation technologies for internal cooling of turbine components of gas turbine engines. *International Journal of Rotating Machinery*, ID 275653. https://doi.org/10.1155/2013/275653

Horlock, J. H., Watson, D. T., & Jones, T. V. (2001). Limitations on gas turbine performance imposed by large turbine cooling flows. *Journal of Engineering for Gas Turbines and Power*, *123*(3), 487–494. https://doi.org/10.1115/1.1373398

Jaiswal, A. K., & Afzal, A. (2023). Design optimization of prismatic rib turbulators in a rectangular channel based on multi-objective criterion. *International Journal of Thermal Sciences*, *185* (March), 108091. https://doi.org/10.1016/j.ijthermalsci.2022.108091

Kim, K. M., Lee, H., Kim, B. S., Shin, S., Lee, D. H., & Cho, H. H. (2009). Optimal design of angled rib turbulators in a cooling channel. *Heat and Mass Transfer*, *45*(12), 1617-1625. https://doi.org/10.1007/s00231-009-0536-3

Koca, F. (2022). Numerical investigation of corrugated channel with backward-facing step in terms of fluid flow and heat transfer. *Journal of Engineering Thermophysics*, *31*(1), 187–199. https://doi.org/10.1134/S1810232822010143

Koca, F., & Güder, T. B. (2022). Numerical investigation of CPU cooling with micro-pin–fin heat sink in different shapes. *The European Physical Journal Plus*, *137* (November), 1276. https://doi.org/10.1140/epjp/s13360-022-03489-7

Lacovides, H., & Launder, B. E. (1995). Computational

fluid dynamics applied to internal gas-turbine blade cooling: A review. *International Journal of Heat and Fluid Flow*, *16*(6), 454-470. https://doi.org/10.1016/0142-727X(95)00072-X

Li, X., Xie, G., Liu, J., & Sunden, B. (2020). Parametric study on flow characteristics and heat transfer in rectangular channels with strip slits in ribs on one wall. *International Journal of Heat and Mass Transfer*, *149* (March), 118396. https://doi.org/10.1016/j.ijheatmasstransfer.2019.07.046

Liu, J., Hussain, S., Wang, W., Xie, G., & Sunden, B. (2021). Experimental and numerical investigations of heat transfer and fluid flow in a rectangular channel with perforated ribs. *International Communications in Heat and Mass Transfer*, *121*(February), 105083. https://doi.org/10.1016/j.icheatmasstransfer.2020.105083

Liu, J., Hussain. S., Wang, J., Wang, L., Xie, G., & Sunden, B. (2018a). Heat transfer enhancement and turbulent flow in a high aspect ratio channel (4:1) with ribs of various truncation types and arrangements. *International Journal of Thermal Sciences*, *123*(January), 99-116. https://doi.org/10.1016/j.ijthermalsci.2017.09.013

Liu, J., Wang, J., Hussain, S., Wang, L., Xie, G., & Sunden, B. (2018b). Application of fractal theory in the arrangement of truncated ribs in a rectangular cooling channel (4:1) of a turbine blade. *Applied Thermal Engineering*, *139*(July), 488-505. https://doi.org/10.1016/j.applthermaleng.2018.04.133

Nagaiah, N. R., & Geiger, C. D. (2014). Evolutionary numerical simulation approach for design optimization of gas turbine blade cooling channels. *International Journal for Simulation and Multidisciplinary Design Optimization*, *5*(A22), 14. https://doi.org/10.1051/smdo/2014001

Ris, V. V., Galaev, S. A., Levchenya, A. M., & Pisarevskii, I. B. (2024). Numerical investigation of a developed turbulent flow and heat transfer in a rectangular channel with single-sided internal ribs. *Thermal Engineering*, *71*, 167–175. https://doi.org/10.1134/S0040601524020083

Singh, P., & Ekkad, S. (2017). Experimental study of heat transfer augmentation in a two-pass channel featuring V-shaped ribs and cylindrical dimples. *Applied Thermal Engineering*, *116*(April), 205–216. https://doi.org/10.1016/j.applthermaleng.2017.01.098

Sunden, B., & Xie, G. (2010). Gas turbine blade tip heat transfer and cooling: a literature survey. *Heat Transfer Engineering*, *31*(7), 527–554. https://doi.org/10.1080/01457630903425320

Tanda, G., Ahmed, E. N., & Bottaro, A. (2023). Natural convection heat transfer from a ribbed vertical plate: effect of rib size, pitch, and truncation. *Experimental Thermal and Fluid Science*, *145* (Julay), 110898. https://doi.org/10.1016/j.expthermflusci.2023.110898

Zhang, G., Liu, J., Sunden, B., & Xie, G. (2021). Combined experimental and numerical studies on flow characteristic and heat transfer in ribbed channels with vortex generators of various types and arrangements. *International Journal of Thermal Sciences*, *167*(September), 107036. https://doi.org/10.1016/j.ijthermalsci.2021.107036

Zheng, S., Liu, G., Zhang, Y., Wang, H., Gao, S., Yang, Y., Li, H., Sunden, B., & Wang, X. (2023). Performance evaluation with turbulent flow and heat transfer characteristics in rectangular cooling channels with various novel hierarchical rib schemes. *International Journal of Heat and Mass Transfer*, *214*(November), 124459. https://doi.org/10.1016/j.ijheatmasstransfer.2023.124459